INTERNATIONAL JOURNAL OF OPTIMIZATION IN CIVIL ENGINEERING
Int. J. Optim. Civil Eng., 2025; 15(4):621-641

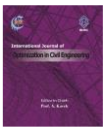

A CASCADE OPTIMIZATION APPROACH USING THE OPTISEARCH ALGORITHM IN CONCRETE FRAME WITH RELIABILITY CONSTRAINTS

A. Kaveh[1*,†], P. Salimi[2], and H.A. Rahimi Bondarabadi[2]
[1]*School of Civil Engineering, Iran University of Science and Technology, Tehran, Iran*
[2]*Department of Civil Engineering, Yazd University, Yazd, Iran*

ABSTRACT

This work investigates the optimization of concrete structures using metaheuristic algorithms-based reliability. One of the major challenges in the optimization of concrete structures is the extensive search domain, which may lead to convergence to local optima and incorrect results. In this study, instead of solely relying on optimization algorithms that are prone to local optima, a novel approach is proposed. Based on the Cascade Algorithm, this method discretized the search domain for section of beam and column dimensions and increased step by step. After each cross-section is created, it is assigned to the corresponding element. Subsequently, structural analysis is performed, and using reliability-based constraints and analysis, the least-cost section for each element is selected. Based on the obtained low-cost sections, the upper and lower bounds for each design variable are then narrowed. Finally, metaheuristic algorithms are applied to determine the optimal cross-sections with high precision. The results demonstrate that this approach significantly reduces the likelihood of falling into local optima and improves both the speed and accuracy of metaheuristic algorithms.

Keywords: Optimization; Concrete frame; OptiSearch; metaheuristic algorithms; reliability; embodied energy.

Received: 23 October 2025; Accepted: 11 December 2025

[*]Corresponding author: School of Civil Engineering, Iran University of Science and Technology, Tehran, Iran
[†]E-mail address: alikaveh@iust.ac.ir (A. Kaveh)

1. INTRODUCTION

Engineering optimization aims to identify optimal solutions for complex problems involving multiple design variables and constraints. A major challenge is navigating large and intricate search spaces. Metaheuristic methods are increasingly applied as effective approaches for searching optimization [1].

Kaveh and Ilchi Ghazan [2] proposed the MDVC-UVPS hybrid algorithm for large-scale dome structures. Various studies have explored RC structure optimization: Govindaraj and Ramasamy [3] optimized continuous beams, Yeo and Gabbai [4] minimized embodied energy, Kaveh and Sabzi [5] reduced costs in RC frames, and Kaveh and Behnam [6] combined CSS algorithms for 3D structures. Kaveh [7] developed ECBO and NSECBO algorithms, Esfandiari et al. [8] proposed DMPSO, Vaez and Qomi [9] optimized shear walls, and Gan et al. [10] introduced GA-based approaches for high-rise structures.

Recent research emphasizes sustainability. Dehnavipour et al. [11] used PSO for code-based designs, Kaveh et al. [7, 12, 13] explored cost and CO_2 minimization and Negrin-Diaz [14] employed Biogeography-Based Optimization.

Salimi et al. [15] and Bondarabadi et al. [16] developed cascade optimization methods. Mottaghi et al. [17] studied cost-CO_2 trade-offs, and Kaveh et al. [18, 19] optimized bridge components and non-prismatic beams. Sustainability research includes Gartner [20], Duxson et al. [21], Paya-Zaforteza et al. [22], de Medeiros et al. [23], Park et al. [24, 25], Eleftheriadis et al. [26] and Yoon et al. [27].

Reliability-based optimization addresses uncertainties [28-30]. Kaveh et al. [31-36] advanced reliability methods using various metaheuristic approaches, accounting for uncertainties in material properties and structural performance.

This study presents a novel cascade optimization approach that efficiently identifies optimal design variable bounds, enabling improved search space exploration and convergence while considering economic, environmental, and reliability objectives.

2. METHODOLOGY

In this study, a cascade optimization algorithm, consisting of a novel approach combined with a metaheuristic method, is introduced and validated through comparison with existing algorithms. Subsequently, a four-story reinforced concrete frame is optimized by establishing a link between MATLAB and SAP2000. The main feature of the proposed algorithm is the restriction of the upper and lower limits of design. Specifically, the approximate ranges of the optimal values for each design variable are initially identified using different techniques (in this study, the trial-and-error method). The search space of each design variable is then restricted to values near the preliminary optima. A schematic illustration of the algorithm's mechanism is provided. Essentially, when a metaheuristic algorithm operates within predefined ranges of design variables that are expected to produce the best objective function value, it is able to achieve the optimal solution more quickly and accurately. This optimization method is referred to as the "OptiSearch Algorithm."

The restricted optimal range can be determined using different approaches, such as trial-and-error, metaheuristic algorithms, or prior knowledge (e.g., deep learning). The proposed algorithm is implemented through the following sequence of steps:

1. Specification of the objective function, constraints, and the number of design variables, initial upper and lower bounds for each variable, initial population, and other required parameters.
2. Generate a set of random numbers within the defined limits, and then evaluate the objective function.
3. Repeat Steps 1 and 2 for the required number of iterations (a greater number of repetitions generally enhances accuracy).
   At this stage, multiple independent lists of numbers are created within the bounds of each variable. The process then continues as follows:
4. Determine the optimal objective function value and its corresponding design variables within each list, based on Step 2.
5. Define new, narrower upper and lower limits in such a way that all design variable values associated with the best objective function in each list are preserved.
6. Repeat Steps 2 through 5 iteratively, gradually tightening the bounds and improving the accuracy of the solution. If the number of iterations reaches the specified limit, or if the difference between the current best solution and the previous one becomes negligible within a predefined tolerance, the solution is regarded as optimal. Otherwise, the latest result serves as the basis for the next iterations. It is clear that increasing the number of repetitions brings the computed solution closer to the global optimum.

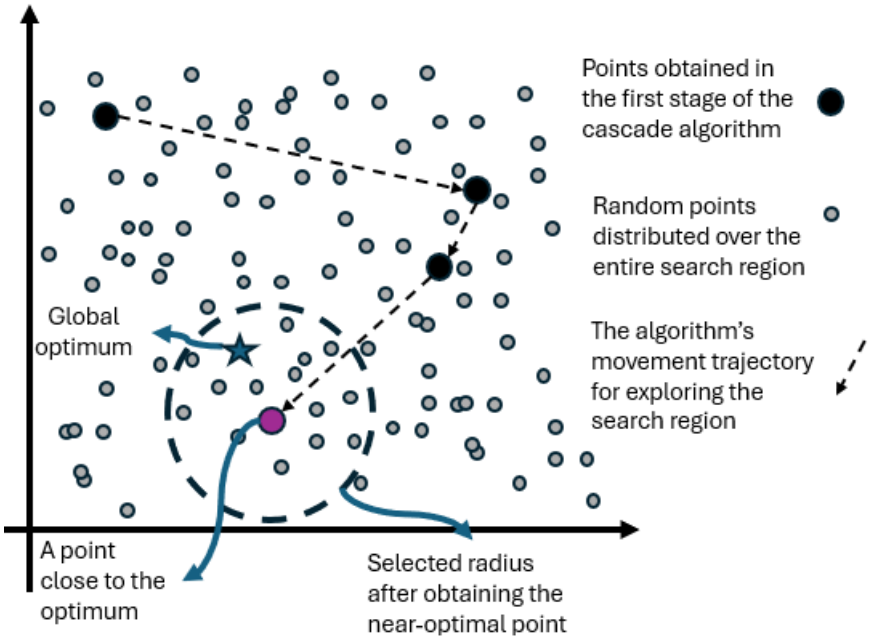

Figure 1: Description of the optimization search algorithm

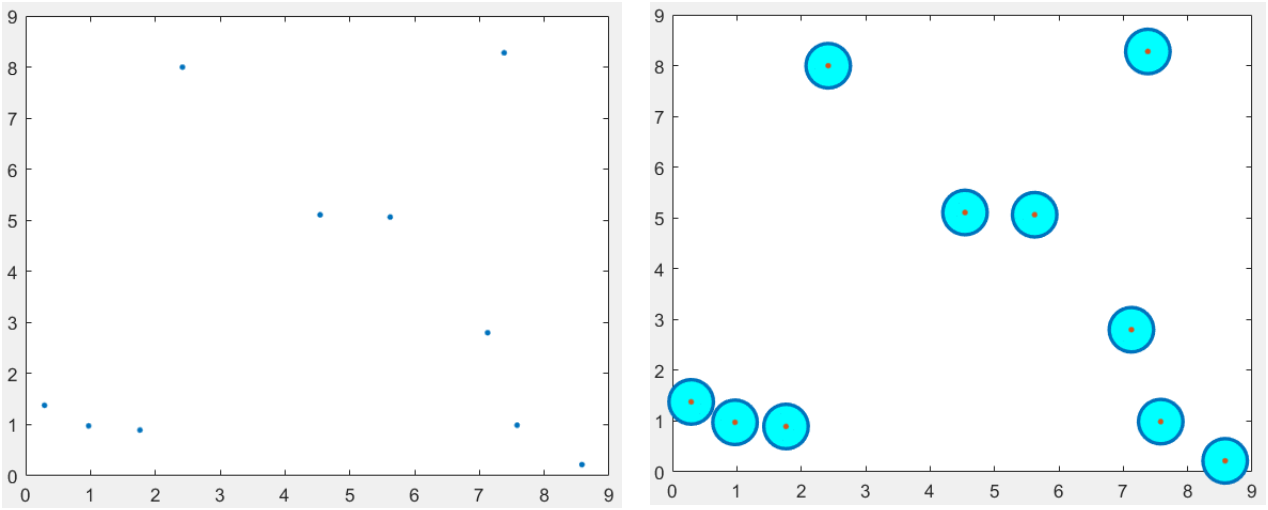

Figure 2: Steps 4 and 5 of the OptiSearch algorithm

Error! Reference source not found. presents a description of the optimization search algorithm, while the blue margin in Figure 2 illustrates the convergence toward the optimal point, which is achieved by progressively restricting the search range of design variables. The proposed algorithm is then evaluated using a set of well-established benchmark optimization problems to assess its efficiency and to compare its performance with existing algorithms.

2.1. Simulation results for a tension/compression string design problem

Belegundu[37] and Arora [38], initially proposed the tension/compression spring design problem, as depicted in Figure 3. The main goal is to reduce the spring's weight while ensuring that constraints on minimum deflection, shear stress, and natural frequency are met.

The problem requires optimizing three key design parameters: the wire diameter (w, x_1), mean coil diameter (d, x_2), and the number of active coils (N, x_3).

The mathematical representation of this optimization task is given below:

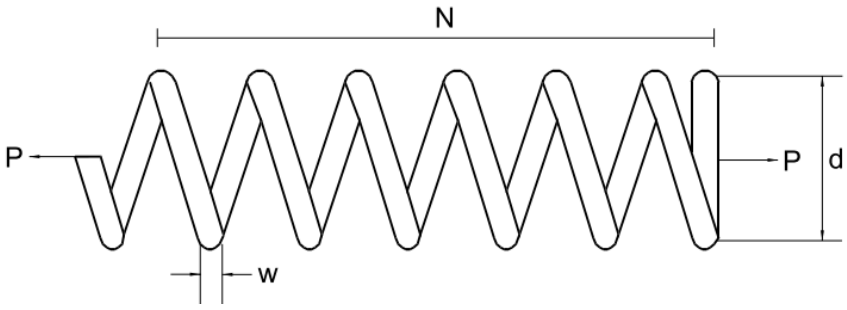

Figure 3: The tension/compression spring design task, highlighting the associated design variables.

$$fcost = (x_3 + 2)x_2x_1^2$$

$$g1 = 1 + \frac{x_2^3 x_3}{71785 x_1^4}$$

$$g2 = \frac{4x_2^2 - x_1 x_2}{12566(x_2 x_1^3 - x_1^4)} + \frac{1}{5108 x_1^2} - 1$$

$$g3 = 1 - \frac{140.45 x_1}{x_2^2 x_3}$$

$$g4 = \frac{x_1 + x_2}{1.5} - 1$$

$$0.05 \leq x_1 \leq 2$$

$$0.25 \leq x_2 \leq 1.3$$

$$2 \leq x_3 \leq 15$$

Notably, the optimal designs obtained in [39] and [40] were found to be infeasible, as both violated the second constraint

Table 1 compares the best results obtained by OptiSearch algorithm with those reported in previous studies.

Notably, the optimal designs obtained in [39] and [40] were found to be infeasible, as both violated the second constraint

Table 1: optimal designs of Simulation results for a tension/compression string design problem obtained by algorithms

Methods	x_1	x_2	x_3	f_{min}
Belegundu [37]	0.05	0.345900	14.25	0.0128334
Arora [38]	0.053396	0.399180	9.185400	0.0127303
Coello [41]	0.051480	0.351661	11.632201	0.127048
Coello & Montes [42]	0.051989	0.363965	10.890522	0.126810
Qie & Wang [43]	0.051728	0.357644	11.244543	0. 126747
Montes & Coello [44]	0.051643	0.355360	11.397926	0.12698
Kaveh & talatahari [39]	0.051865	0.361500	11	0.126432
Abualigah et al. [40]	0.0502	0.3526	10.5425	0.011165
OptiSearch algorithm	0.0517	0.3579	11.2198	0.126661

2.2. Simulation results for a pressure vessel design problem

In the second example, the focus is on reducing the total cost associated with manufacturing a cylindrical pressure vessel, as shown in Fig. 5. This design problem has been widely studied, and a variety of heuristic approaches have been employed for its optimization.

The system is characterized by four design variables, two of which are discrete and two continuous, and must satisfy four inequality constraints. The variables include the thickness

of the cylindrical shell (T_S, x_1), the thickness of the spherical head (T_h, x_2), the radius of the shell (R, x_3), and the length of the shell (L, x_4). Thicknesses of both the shell and the head are restricted to multiples of 0.0625 inches, ranging from 0.0625 to 6.1875 inches. The radius and length of the cylinder are limited to values between 10 and 200 inches.

The mathematical formulation of this optimization problem is presented below:

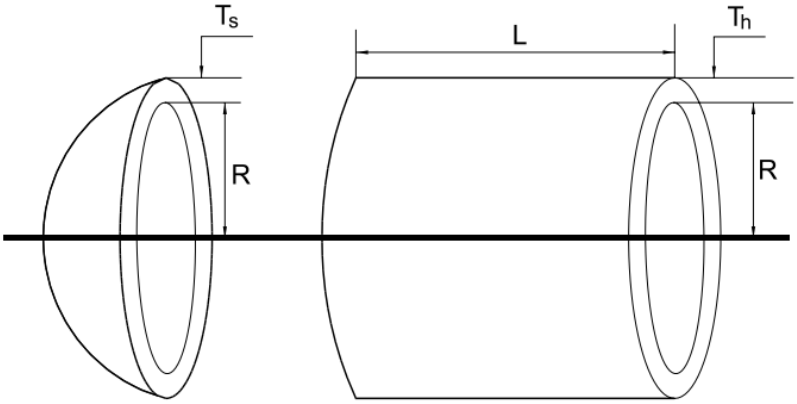

Figure 4: Pressure vessel design problem with four design variables

$$fcost = 0.6224x_1x_3x_4 + 1.7781x_2x_3^2 + 3.1661x_1^2x_4 + 19.84x_1^2x_3$$

$$g1 = -x_1 + 0.0193x_3$$

$$g2 = -x_2 + 0.00954x_3$$

$$g3 = -\pi x_3^2 x_4 - \frac{4}{3}\pi x_3^3 + 1296000$$

$$g4 = x_4 - 240$$

$$0 \leq x_1 \leq 99$$

$$0 \leq x_2 \leq 99$$

$$10 \leq x_3 \leq 200$$

$$10 \leq x_4 \leq 200$$

As indicated in Table 2, the OptiSearch method delivered the best results for the pressure vessel optimization task.

As evident from the given results, the solutions computed by this algorithm are more accurate, and the objective function has improved significantly. In the following section, the optimization of a structural example is discussed.

Table 2Table 2: optimal designs of Simulation results for a pressure vessel design problem obtained by algorithms

Methods	x_1	x_2	x_3	x_4	f_{min}
Sandgren [45]	1.125000	0.625000	47.700000	117.701000	8,129.1036
Kannan & Kramer [46]	1.125000	0.625000	58.291000	43.690000	7,198.0428
Deb [47]	0.937500	0.500000	48.329000	112.679000	6,410.3811
Coello [41]	0.812500	0.437500	40.323900	200.000000	6,288.7445
Coello & Montes [42]	0.812500	0.437500	42.097398	176.654050	6,059.9463
Qie & Wang [43]	0.812500	0.437500	42.091266	176.746500	6061.0777
Montes & Coello [44]	0.812500	0.437500	42.098087	176.640518	6059.7456
Kaveh & talatahari [39]	0.812500	0.437500	42.098353	176.637751	6059.7258
Abualigah et al. [40]	1.0540	0.182806	59.6219	38.8050	5949.2258
OptiSearch algorithm	0.7788	0.3849	40.3503	199.5729	5886.3830

2.4. Concrete frame example

This section focuses on the optimization of a four-story, two-bay reinforced concrete frame, depicted in Figure 5, subjected to the loading condition given in **Error! Reference source not found.**. The optimization is carried out using the cascade optimization algorithm, aiming to simultaneously minimize two objectives: the total cost and the embodied energy. The design must satisfy both deterministic and probabilistic constraints, as outlined in the objective function section.

Embodied energy is the cumulative amount of energy required across the entire life cycle of building materials, encompassing raw material extraction, manufacturing, transportation, and construction. In the case of the reinforced concrete frame considered here, this includes the energy required for concrete production, steel reinforcement fabrication, and the processes of construction, transportation, and installation.

The **OptiSearch** algorithm, with minor modifications based on the problem characteristics, was employed for the optimization process. The strategy from [24] was employed to narrow the search space of the design variables. In contrast to [24], where the aspect ratio was defined as the moment ratio of axis 3 to axis 2 (Figure 6), such a formulation was not feasible here owing to the 2D configuration of the frame. In this case, $M_3 = 0$, and cross-sectional dimensions were therefore determined based solely on M_2.

According to Figure 7 and Table 3, Section depths were selected from predefined discrete values, while widths were computed according to the problem constraints and rounded upward to the nearest multiple of five, ensuring selection from the same table. The resulting cross-sections were not necessarily square and were determined according to the governing relationships.

Constraining the upper and lower limits of each element substantially reduces the search space. This reduction enhances the efficiency of the metaheuristic algorithm, allowing it to locate the optimal solution with greater speed and precision. Consequently, the optimization procedure becomes faster, and the quality of the obtained results improves.

The equivalent static analysis is performed using the load combinations specified in **Error! Reference source not found.**, which are derived from the ACI 318-08 code. The data of earthquake [48], loading [48] and materials [49] are shown in Table 4.

Table 3: Selected values for beam and column cross-sectional dimensions

Selected depth of beam and column cross-sections
30-35-40-45-50-55-60-65-70-75-80-85-90

Table 4 to
Table *6*. Table 7 presents the price and embodied energy of materials and formwork. In addition, the parameters f_c', f_y and the cross-sectional dimensions of each beam and column are treated as probabilistic variables, each assigned a coefficient of variation (CV) of 0.1. The mean values for material properties (f_c' and f_y) correspond to those specified in
Table 6, while for cross-sectional dimensions, the mean values represent those selected by the optimization algorithm at each iteration.

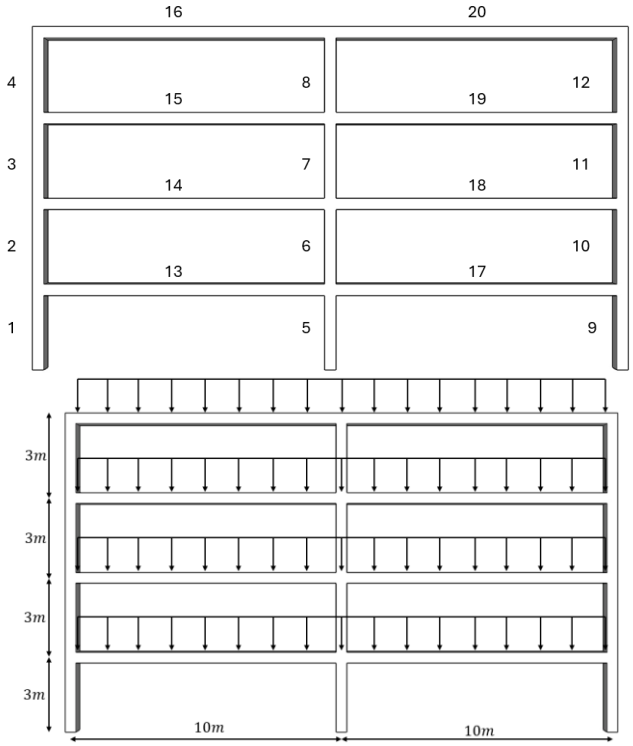

Figure 5 The 4-story RC frame with the height and span of 3 m and 10 m respectively in each story

$$Q = \begin{cases} 1.2D + 1.6L \\ 1.2D + L \pm 1.4E \\ 0.9D \pm 1.4E \end{cases} \quad (1)$$

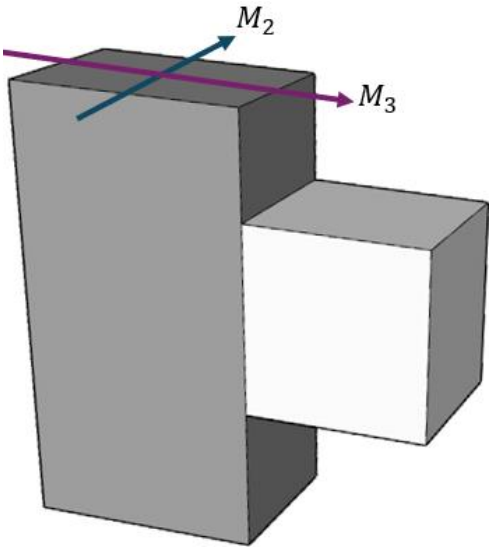

Figure 6: The applied bending moments on the column section

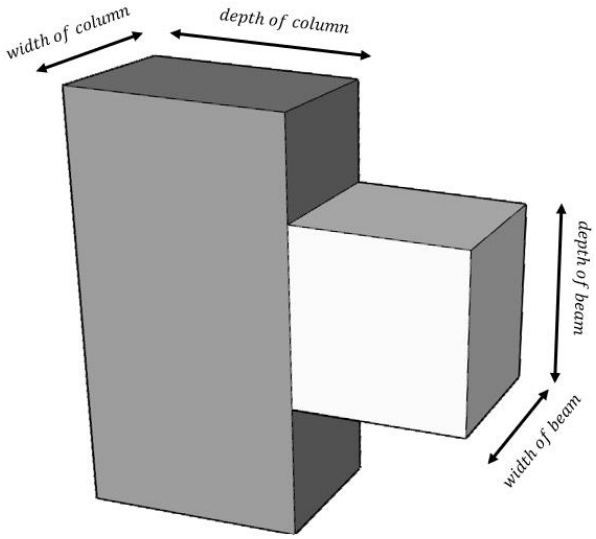

Figure 7: Depth and width of beam and column cross-sections

Table 3: Selected values for beam and column cross-sectional dimensions

Selected depth of beam and column cross-sections
30-35-40-45-50-55-60-65-70-75-80-85-90

Table 4: Earthquake parameter

Base shear Coefficient (C)	**Building Height Exponent (K)**
0.1074	1.044

Table 5: Loading

Load	***N,m***
Dead	$22.3kNm$
Live	$10.7kNm$

Table 6: Material

Materials	**Strength**
concrete	$f_c' = 27.579\ MPa$
Steel of rebars	$f_y = 344.7379\ MPa$ $f_u = 620.5282\ MPa$ $f_{ye} = 455.054\ MPa$ $f_{ue} = 682.581\ MPa$

Table 7: price and embodied energy of materials and formwork

Unit	**Cost €**	**Embodied energy (MJ/kg)[50]**	**Specific weight (kg/m^3)**

Steel B-500	Kg	1.3	36.4	7850
Concrete	m^3	105.17	1.11	2300
Form work	m^2	22.75	-	-

In the sections that follow, the objective function, the problem's constraints, and the detailed procedure of the proposed algorithm are outlined.

2.4.1. Definition of the objective function and deterministic/probabilistic

The objective function is formulated as follows, **Error! Reference source not found.**, and is optimized under both deterministic and probabilistic constraints. Probabilistic parameters such as f_c', f_y, and the cross-sectional dimensions of beams and columns are modeled as random variables. Accordingly, constraints that include these parameters are regarded as probabilistic, whereas the remaining constraints are considered deterministic. The reliability index is assumed to have a value of 2.5 [28].

$$\begin{aligned} minimize: \quad & objective\ functions(d) \\ subject\ to: \quad & \beta(d,x) \geq \beta^{target} \quad i = 1,2,\dots,m \\ & g_j(x) \leq 0 \quad j = m+1,\dots,n \end{aligned} \tag{2}$$

2.4.2. Definition of the objective function and penalty

To ensure that all constraints in the optimization problem are satisfied, a penalty function is incorporated into the objective function, as expressed as **Error! Reference source not found.**. Here, k is a large positive constant, and in this study, it is set to 10^7.

$$f = f \times (1 + \sum Penalty)^k \tag{3}$$

2.4.3. Objective function

The optimization problem in this section involves two objectives: minimizing cost and minimizing embodied energy, the latter reflecting energy consumption throughout manufacturing and construction. Since the algorithm is designed for single-objective problems, the bi-objective formulation is transformed by equally weighting both objectives (0.5 each), resulting in a single combined objective function.
Table 8 summarizes the parameters used in the objective functions f_1 and f_2.

$$f_1 = \sum \begin{matrix} A_s^{beam} \times L_{beam} \times \gamma_s \times C_s + \\ (depth_{beam} \times width_{beam} - A_s^{beam}) \times L_{beam} \times C_c \\ 2 \times (depth_{beam} + width_{beam}) \times L_{beam} \times C_f \end{matrix} + \sum \begin{matrix} A_s^{column} \times L_{column} \times \gamma_s \times C_s + \\ (depth_{column} \times width_{column} - A_s^{column}) \times L_{column} \times C_c \\ 2 \times (depth_{column} + width_{column}) \times L_{column} \times C_f \end{matrix}$$

$$f_2 = \sum \begin{matrix} A_s^{beam} \times L_{beam} \times \gamma_s \times EM_s + \\ (depth_{beam} \times width_{beam} - A_s^{beam}) \times L_{beam} \times EM_c \end{matrix} + \sum \begin{matrix} A_s^{column} \times L_{column} \times \gamma_s \times EM_s + \\ (depth_{column} \times width_{column} - A_s^{column}) \times L_{column} \times EM_c \end{matrix}$$

Table 8: Specifications of Parameters Used in the Objective Functions

Reinforcement area of beam $\boldsymbol{A_s^{beam}}$	Beam length $\boldsymbol{L_{beam}}$	Reinforcement area of column $\boldsymbol{A_s^{column}}$	Column length $\boldsymbol{L_{column}}$
Beam depth $\boldsymbol{depth_{beam}}$	Beam width $\boldsymbol{width_{beam}}$	Column depth $\boldsymbol{depth_{column}}$	Column width $\boldsymbol{width_{column}}$
Reinforcement cost $\boldsymbol{C_s}$	Concrete cost $\boldsymbol{C_c}$	Formwork cost $\boldsymbol{C_f}$	
Reinforcement density $\boldsymbol{\gamma_s}$	Embodied energy of reinforcement $\boldsymbol{EM_s}$	Embodied energy of concrete $\boldsymbol{EM_c}$	

Table 9: Cost and Embodied Energy of Materials and Formwork

Material	**Unit**	**Cost (€)**	**Embodied Energy (MJ/kg)[50]**	**Density (kg/m^3)**
Steel B-500	Kg	1.3	36.4	7850
Concrete	m^3	105.17	1.11	2300
Formwork	m^2	22.75	-	-

2.4.4. Constraints

The following constraints are considered for the optimization of the two objective functions.

$$g_1 = \frac{h_{b\,i+1}}{h_{b\,i}} - 1 \leq 0 \qquad g_2 = \frac{b_{b\,i+1}}{b_{b\,i}} - 1 \leq 0 \qquad g_3 = \frac{h_{c\,i+1}}{h_{c\,i}} - 1 \leq 0$$

$$g_4 = \frac{b_{c\,i+1}}{b_{c\,i}} - 1 \leq 0 \qquad g_5 = \frac{db_{c\,i+1}}{db_{c\,i}} - 1 \leq 0 \qquad g_6 = \frac{ndb_{c\,i+1}}{ndb_{c\,i}} - 1 \leq 0$$

$$g_7 = \frac{As_{b,min,i}}{As_{b,i}} - 1 \leq 0 \qquad g_8 = \frac{As_{b,i}}{As_{b,max,i}} - 1 \leq 0 \qquad g_9 = \frac{Av_{b,min,i}}{Av_{b,i}} - 1 \leq 0$$

$$g_{10} = \frac{As_{c,min,i}}{As_{c,i}} - 1 \leq 0 \qquad g_{11} = \frac{As_{c,i}}{As_{c,max,i}} - 1 \leq 0 \qquad g_{12} = \frac{\frac{Av_c}{S} min, i}{\frac{Av_c}{S} i} - 1 \leq 0$$

$$g_{13} = \frac{Av_{c,min,i}}{Av_{c,i}} - 1 \leq 0 \qquad g_{14} = \frac{S_{b,min,i}}{S_{b,i}} - 1 \leq 0 \qquad g_{15} = \frac{S_{b,i}}{S_{b,max,i}} - 1 \leq 0$$

$$g_{16} = \frac{S_{c,min,i}}{S_{c,i}} - 1 \leq 0 \qquad g_{17} = \frac{S_{c,i}}{S_{c,max,i}} - 1 \leq 0 \qquad g_{18} = \frac{M_{u,b}}{\emptyset M_{u,b}} - 1 \leq 0$$

$$g_{19} = \frac{M_{u,c}}{\emptyset M_{u,c}} - 1 \leq 0 \qquad g_{20} = \frac{V_{u,b}}{\emptyset V_{u,b}} - 1 \leq 0 \qquad g_{21} = \frac{V_{u,c}}{\emptyset V_{u,c}} - 1 \leq 0$$

$$g_{22} = \frac{P_{u,c}}{\emptyset P_{u,c}} - 1 \leq 0$$

2.4.5. Cascade algorithm procedure for optimization

Initially, a list of cross-sections for the column elements is generated, where the smallest value from the Table 3 is selected for the column depth, and the corresponding width is considered to be less than or equal to the depth. Table *10* illustrates the procedure of Step 1. The code-specified limitation for column dimensions, as defined by Figure 8 and **Error! Reference source not found.**, is satisfied given the range of values used in this study.

Table 10: Selected Depths and Widths for Column Cross Sections

Selected Column Depth (cm)	**35**	**40**	**45**	**90**
	35	35	35	35
		40	40	40
Corresponding Widths			45	45
				⋮
				90

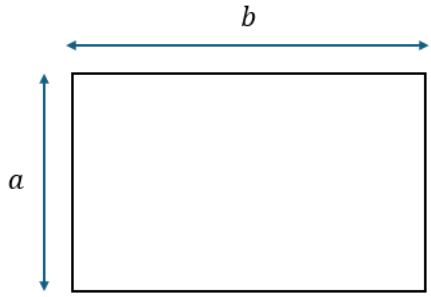

Figure 8: Schematic of Column Length and Width

$$a \geq \max(0.3b\,, 25\ cm)$$
$$b \geq \max(0.3a\,, 25\ cm) \tag{4}$$

In the following, the subsequent steps of the algorithm are described.

1. By assigning each cross-section to the corresponding column, the required reinforcement is computed, and the objective function value is evaluated.

2. Cross-sections for which the required reinforcement ratio for each column lies between 1% and 4% are stored. This step ensures economic efficiency: sections that are overly large (requiring less than 1% reinforcement) are excluded, as are sections that are too small (exceeding 4% reinforcement). Large sections satisfy code constraints but result in higher objective function values, whereas small sections may violate code requirements. At this stage, the first step of the optimization places the column design in the "to be designed" state in ETABS. According to Table 10, 78 column cross-sections are available; however, for some columns, particularly upper columns with lower applied forces, evaluating all 78 sections is unnecessary. Once a section yields a 1% reinforcement ratio, the next section is not evaluated unless it represents the last width for a given depth, in which case the next depth is considered, and the corresponding results are extracted and compared with other sections.

3. Among the stored cross-sections, the one with the most favorable objective function is selected. This procedure also satisfies the constraint that upper columns do not exceed the dimensions of lower columns.

4. After determining column cross-sections, beam cross-sections are selected. According to Figure 9, the beam width depends on the widths of the connected columns. Since each beam in the frame is connected to two columns, the smaller of the two column widths is used for selecting the beam width. The minimum allowable width from the Table 3 is taken as the smallest width, and the beam depth is set to be greater than or equal to the selected width. Code limitations for beam dimensions, defined by Figure 9 and **Error! Reference source not found.** and **Error! Reference source not found.**, are satisfied given the range of values used in this study.

5. Based on Table 11 and the minimum widths of the connected columns, the beam width is selected, and cross-sections with permissible depths for that width are generated and assigned. For some beams, evaluating all permissible sections is unnecessary; once a section yields a reinforcement ratio below the minimum code requirement, the next section is not evaluated unless it represents the last width for a given depth, in which case the next depth is considered. The results for each evaluated section are then extracted and compared with other sections.

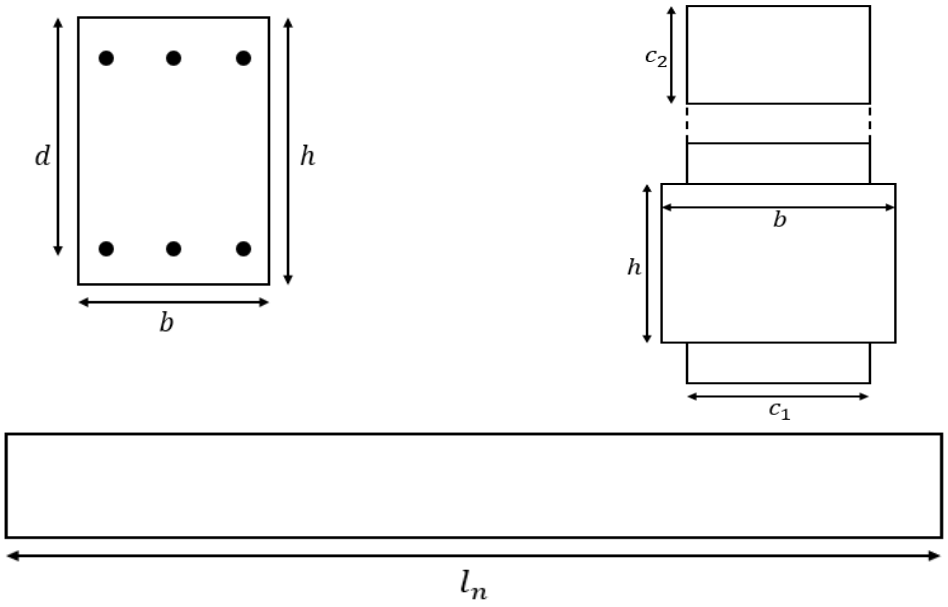

Figure 9: Schematic of Beams, Columns, and Their Connections

$$d \leq \frac{l_n}{4} \tag{5}$$

$$b \geq \max\left(\frac{h}{4}, 25\ cm\right)$$

$$b \leq \left\{c_1 + 2 \times \frac{3}{4}h\right\} \tag{6}$$

$$b \leq \left\{c_1 + 2 \times \frac{1}{4}c_2\right\}$$

Table 11: Selected Depths and Widths for beam Cross Sections

Selected beam Depth (cm)	35	40	45	...	90
Corresponding Widths	35 40 45 ⋮ 90	40 45 ⋮ 90	45 ⋮ 90	...	90

It should be noted that the duration of Steps 3 and 5 can be reduced by applying constraints, such as limiting the length-to-width ratio of cross-sections, since the primary purpose of these steps is to reduce the search space and narrow the initial upper and lower bounds. In this study, no such constraints are applied to increase problem accuracy.

6. Cross-sections that satisfy all code requirements are stored in the allowable section matrix. The constraint that the beam width must not exceed the widths of the connected columns is also considered.
7. Among the stored cross-sections, the one yielding the most favorable objective function is selected.

Since the selection of column sections is performed while beam sections remain fixed, and then beam sections are selected once the column sections are determined, Steps 1 through 7 are repeated until no further changes occur in the sections, achieving convergence.

Upon completion of the algorithm steps, the obtained cross-sections fall within the optimal range. The cross-sections allow the search space of each structural element to be limited, thereby enhancing the speed of optimization. The level of this limitation is chosen based on the preferred balance between precision and processing time. It should be noted that at this stage, reliability is not considered, and all parameters are treated as deterministic, taking their mean values. Table 12 and Table 13 present the near-optimal cross-sections for columns and beams, respectively.

Defining the upper and lower bounds of each element through these cross-sections enables the metaheuristic algorithm to begin the optimization process with improved efficiency and precision. Each obtained cross-section serves as the center of the new upper and lower bounds with a specified radius—in this study, 10 cm. Since the steps taken to estimate the approximate cross-section dimensions are based on deterministic optimization and these dimensions may differ significantly from the deterministic optimum in reliability analysis, the deterministic cross-sections are instead used as initial points for the metaheuristic algorithm in the reliability-based analysis, rather than defining a radius.

Table 12: near-optimal cross-sections for columns

Name of columns	Width (cm)	Depth (cm)	Rebar (mm)	Number of rebar
1	45	65	25	6
2	45	65	25	5
3	40	50	25	3
4	40	50	25	3
5	60	85	28	6
6	60	85	28	6
7	45	65	25	6
8	45	65	25	5
9	60	85	28	6
10	50	70	25	6
11	45	65	25	5
12	45	65	25	5

Table 14 and

Table *15* present the deterministic optimal cross-sections of columns and beams, respectively. These sections are obtained by applying the technique of narrowing the upper and lower bounds and removing unnecessary regions within the search space.

Table 16 and Table 17 show the reliability-based optimal cross-sections for columns and beams, respectively. Compared to deterministic optimal sections, the reliability-based optimal sections are generally stronger to ensure the required reliability, as evident from the comparison between Table 14 and Table 16, and

Table 15 and Table 17.

It should be noted that for the column depth, the minimum required reinforcement is used to facilitate construction. Figure 10 illustrates Column 1 from Table 14.

Table 13: near-optimal cross-sections for beams

Name of beams	Width (cm)	Depth (cm)
13	35	70
14	40	75
15	40	70
16	35	65
17	35	70
18	40	75
19	35	65
20	35	55

Table 14: deterministic optimal cross-sections of columns

Name of columns	Width (cm)	Depth (cm)	Longitudinal Rebar (mm)	Number of rebar	Confinement Rebar (mm)	Longitudinal spacing of confinement bars (cm)	f-cost	f-Embodied energy
1	46	67	25	6	12	21.5	338881.1	40557.17
2	41	64	25	5	14	29.5	290205.6	35814.20
3	37	48	25	3	10	29.5	199285.5	25669.62
4	37	48	25	3	10	31	199285.5	25668.88
5	61	83	28	6	16	29.5	551380.1	52610.26
6	61	83	28	6	16	31	551380.1	52608.38
7	46	67	25	6	12	30.9	338880.6	40543.68
8	41	64	25	5	14	30.9	290205.3	35806.94
9	61	83	28	6	16	29.5	551380.1	52610.26
10	46	67	25	6	12	29.5	338880.8	40549.02
11	41	64	25	5	14	31	290205.5	35812.76
12	41	64	25	5	14	30.9	290205.3	35806.94

Table 15: deterministic optimal cross-sections of beams

Name of beams	Width (cm)	Depth (cm)	Longitudinal Rebar (mm)	Number of rebar (top)	Number of rebar (bottom)	Confinement Rebar (mm)	Longitudinal spacing of confinement bars (cm)	f-cost	f-Embodied energy

13	39	68	18	12	5	10	14.4	294063.8	34547.9
14	41	74	25	6	4	10	17.25	335125.1	38065.5
15	39	68	18	12	5	12	14.4	294064.3	34561.6
16	32	62	22	9	5	14	14.25	220525.6	34331.6
17	39	68	18	11	6	10	14.4	294063.8	34547.9
18	41	74	22	8	7	14	17.25	334372.7	40348.3
19	3۷	6۸	28	6	5	14	14.25	219147.3	38462.7
20	31	53	18	11	4	10	12	184290.8	27845.6

Table 16: the reliability-based optimal cross-sections for columns

Name of columns	Width (cm)	Depth (cm)	Longitudinal Rebar (mm)	Number of rebar	Confinement Rebar (mm)	Longitudinal spacing of confinement bars (cm)	f-cost	f-Embodied energy
1	60	71	32	6	16	23.9	462440.91	55827.27
2	41	67	32	5	10	16.7	300705.41	45407.35
3	41	52	32	4	10	16.7	234853.37	37446.44
4	41	49	32	3	10	34.5	222904.47	32177.78
5	70	89	32	8	16	19.1	671611.19	72221.54
6	62	80	32	7	16	26	536512.22	63157.62
7	60	71	32	6	14	26.9	462440.32	55810.87
8	46	71	32	6	12	30.9	355380.92	52175.74
9	72	80	32	7	16	24	622448.36	65849.30
10	62	77	32	6	14	16.7	517938.42	57841.38
11	56	71	32	6	16	25.9	431852.46	54787.29
12	56	71	32	6	14	31.9	431851.86	54770.50

Table 17: the reliability-based optimal cross-sections for beams

Name of beams	Width (cm)	Depth (cm)	Longitudinal Rebar (mm)	Number of rebar (top)	Number of rebar (bottom)	Confinement Rebar (mm)	Longitudinal spacing of confinement bars (cm)	f-cost	f-Embodied energy
13	41	71	20	14	6	12	13.7	320344.7	41322.2
14	43	77	28	8	5	10	16.1	362217.1	48087.1
15	41	71	20	14	6	14	13.4	320345.4	41340.7
16	34	65	22	11	6	16	14.1	244111.7	38748.1
17	41	71	20	13	6	10	13.4	320642.6	40414.3
18	43	77	25	10	7	16	16.2	361895.7	49098.1
19	34	65	28	8	5	14	13.1	242646.4	43124.2
20	33	56	20	12	4	12	10	205603.0	32442.9

Since reliability-based analysis or optimization using metaheuristic algorithms, especially for large and complex problems, is very time-consuming, and the computational time for reliability-based optimization increases significantly, the method of restricting the search space for each design variable can greatly reduce computational effort. As observed from the results, deterministic optimal sections, which are calculated faster by narrowing the search space compared to other methods, serve as the starting points for restricting the search space

in reliability-based optimization. The extent of this restriction can be adjusted according to user preference. In this study, the search space was defined 10 cm above and below the deterministic optimal point.

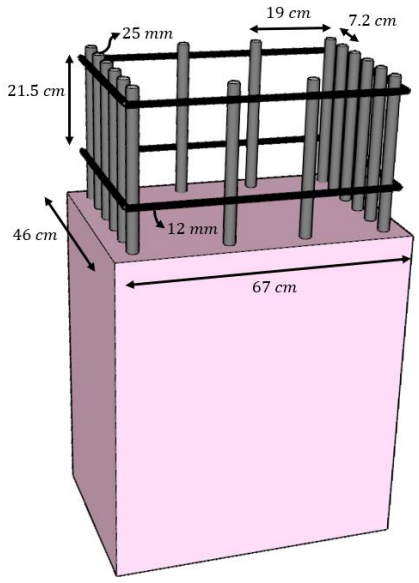

Figure 10: Column 1 from Table 14

3. CONCLUSION

Complex optimization problems are often solved using metaheuristic algorithms, which explore the solution space while respecting variable bounds and problem constraints. The success of these methods is strongly affected by the quality of the initial guess, as starting closer to the optimal solution can significantly enhance the algorithm's efficiency.

The study presents the OptiSearch algorithm, which works by defining upper and lower bounds for the design variables. The algorithm was implemented on a four-story, two-bay frame to achieve optimal safety under constraints based on reliability. Key findings of this study indicate that the OptiSearch algorithm not only converges faster but also provides better results compared to traditional metaheuristic methods. By restricting the search space using defined bounds for the design variables, the algorithm is capable of identifying more accurate solutions. Incorporating reliability constraints ensures that structural safety requirements are satisfied while minimizing material usage and overall costs. Consequently, the OptiSearch algorithm emerges as a promising tool for structural engineering optimization. Its ability to converge rapidly and accurately to an optimal solution represents a significant advancement in structural optimization and offers a viable alternative to conventional metaheuristic approaches.

REFERENCES

1. Kaveh A. *Applications of Metaheuristic Optimization Algorithms in Civil Engineering*. Springer; 2017.
2. Kaveh A, Ilchi Ghazaan M. A new hybrid meta-heuristic algorithm for optimal design of large-scale dome structures. *Engineering Optimization*. 2018;**50**(2):235–52.
3. Govindaraj V, Ramasamy J. Optimum detailed design of reinforced concrete continuous beams using genetic algorithms. *Computers & Structures*. 2005;**84**(1–2):34–48.
4. Yeo D, Gabbai RD. Sustainable design of reinforced concrete structures through embodied energy optimization. *Energy and Buildings*. 2011;**43**(8):2028–33.
5. Kaveh A, Sabzi O. Optimal design of reinforced concrete frames using big bang-big crunch algorithm. *International Journal of Civil Engineering*. 2012;**10**(3):189–200.
6. Kaveh A, Behnam A. Design optimization of reinforced concrete 3D structures considering frequency constraints via a charged system search. *Scientia Iranica*. 2013;**20**(3):387–96.
7. Kaveh A. Cost and CO2 emission optimization of reinforced concrete frames using enhanced colliding bodies optimization algorithm. In: *Applications of Metaheuristic Optimization Algorithms in Civil Engineering*. Springer; 2016:319–50.
8. Esfandiari MJ, et al. Optimum design of 3D reinforced concrete frames using DMPSO algorithm. *Advances in Engineering Software*. 2018;**115**:149–60.
9. Vaez SRH, Qomi HS. Bar layout and weight optimization of special RC shear wall. *Structures*. 2018. Elsevier.
10. Gan VJ, et al. Parametric modelling and evolutionary optimization for cost-optimal and low-carbon design of high-rise reinforced concrete buildings. *Advanced Engineering Informatics*. 2019;**42**:100962.
11. Dehnavipour H, et al. Optimization-based design of 3D reinforced concrete structures. *Journal of Soft Computing in Civil Engineering*. 2019;**3**(3):95–106.
12. Kaveh A, Izadifard R, Mottaghi L. Optimal design of planar RC frames considering CO2 emissions using ECBO, EVPS and PSO metaheuristic algorithms. *Journal of Building Engineering*. 2020;**28**:101014.
13. Kaveh A, Mottaghi L, Izadifard RA. Optimization of columns and bent caps of RC bridges for cost and CO2 emission. *Periodica Polytechnica Civil Engineering*. 2022;**66**(2):553–63.
14. Negrin-Diaz I, Chagoyén-Méndez E, Negrin-Montecelo A. Parameter tuning in the process of optimization of reinforced concrete structures. *Dyna*. 2021;**88**(216):87–95.
15. Salimi P, Boderabady HR, Kaveh A. Optimal design of reinforced concrete frame structures using cascade optimization method. *Periodica Polytechnica Civil Engineering*. 2022;**66**(4):1220–33.
16. Bondarabadi HAR, Kaveh A, Salimi P. Optimal design of shear walls for minimizing the structural torsion using cascade optimization algorithm. *Periodica Polytechnica Civil Engineering*. 2024.
17. Mottaghi L, Izadifard RA, Kaveh A. Factors in the relationship between optimal CO2 emission and optimal cost of the RC frames. *Periodica Polytechnica Civil Engineering*. 2021;**65**(1):1–14.

18. Kaveh A, Mottaghi L, Izadifard R. An integrated method for sustainable performance-based optimal seismic design of RC frames with non-prismatic beams. *Scientia Iranica*. 2021;**28**(5):2596–612.
19. Kaveh A, Mottaghi L, Izadifard R. Sustainable design of reinforced concrete frames with non-prismatic beams. *Engineering with Computers*. 2022;**38**(1):69–86.
20. Gartner E. Industrially interesting approaches to "low-CO2" cements. *Cement and Concrete Research*. 2004;**34**(9):1489–98.
21. Duxson P, et al. The role of inorganic polymer technology in the development of 'green concrete'. *Cement and Concrete Research*. 2007;**37**(12):1590–97.
22. Paya-Zaforteza I, et al. CO2-optimization of reinforced concrete frames by simulated annealing. *Engineering Structures*. 2009;**31**(7):1501–08.
23. de Medeiros GF, Kripka M. Optimization of reinforced concrete columns according to different environmental impact assessment parameters. *Engineering Structures*. 2014;**59**:185–94.
24. Park HS, Hwang JW, Oh BK. Integrated analysis model for assessing CO2 emissions, seismic performance, and costs of buildings through performance-based optimal seismic design with sustainability. *Energy and Buildings*. 2018;**158**:761–75.
25. Park HS, et al. Evaluation of the influence of design factors on the CO2 emissions and costs of reinforced concrete columns. *Energy and Buildings*. 2014;**82**:378–84.
26. Eleftheriadis S, et al. Investigating relationships between cost and CO2 emissions in reinforced concrete structures using a BIM-based design optimisation approach. *Energy and Buildings*. 2018;**166**:330–46.
27. Yoon YC, et al. Sustainable design for reinforced concrete columns through embodied energy and CO2 emission optimization. *Energy and Buildings*. 2018;**174**:44–53.
28. Aoues Y, Chateauneuf A. Benchmark study of numerical methods for reliability-based design optimization. *Structural and Multidisciplinary Optimization*. 2010;**41**(2):277–94.
29. Kalatjari V, Kaveh A, Mansoorian P. System reliability assessment of redundant trusses using improved algebraic force method and artificial intelligence. 2011.
30. Nowak AS, Collins KR. *Reliability of Structures*. CRC Press; 2012.
31. Kaveh A, Ilchi Ghazaan M. Structural reliability assessment utilizing four metaheuristic algorithms. *International Journal of Optimization in Civil Engineering*. 2015;**5**(2):205–25.
32. Kaveh A, Dadras Eslamlou A. An efficient method for reliability estimation using the combination of asymptotic sampling and weighted simulation. *Scientia Iranica*. 2019;**26**(4):2108–22.
33. Kaveh A, Javadi SM, Moghanni RM. Reliability analysis via an optimal covariance matrix adaptation evolution strategy: emphasis on applications in civil engineering. *Periodica Polytechnica Civil Engineering*. 2020;**64**(2):579–88.
34. Kaveh A, Hamedani KB, Kamalinejad M. Set theoretical variants of optimization algorithms for system reliability-based design of truss structures. *Periodica Polytechnica Civil Engineering*. 2021;**65**(3):717–29.
35. Kaveh A, et al. Heuristic operator for reliability assessment of frame structures. *Periodica Polytechnica Civil Engineering*. 2021;**65**(3):702–16.
36. Kaveh A, Zaerreza A. A new framework for reliability-based design optimization using metaheuristic algorithms. *Structures*. 2022. Elsevier.

37. Belegundu AD. A study of mathematical programming methods for structural optimization. 1983.
38. Arora JS. *Introduction to Optimum Design*. Elsevier; 2004.
39. Kaveh A, Talatahari S. An improved ant colony optimization for constrained engineering design problems. *Engineering Computations*. 2010;**27**(1):155–82.
40. Abualigah L, et al. Aquila optimizer: a novel meta-heuristic optimization algorithm. *Computers & Industrial Engineering*. 2021;**157**:107250.
41. Coello CAC. Use of a self-adaptive penalty approach for engineering optimization problems. *Computers in Industry*. 2000;**41**(2):113–27.
42. Coello CAC, Montes EM. Constraint-handling in genetic algorithms through the use of dominance-based tournament selection. *Advanced Engineering Informatics*. 2002;**16**(3):193–203.
43. He Q, Wang L. A hybrid particle swarm optimization with a feasibility-based rule for constrained optimization. *Applied Mathematics and Computation*. 2007;**186**(2):1407–22.
44. Mezura-Montes E, Coello CAC. An empirical study about the usefulness of evolution strategies to solve constrained optimization problems. *International Journal of General Systems*. 2008;**37**(4):443–73.
45. Sandgren E. Nonlinear integer and discrete programming in mechanical design. In: *International Design Engineering Technical Conferences and Computers and Information in Engineering Conference*. American Society of Mechanical Engineers; 1988.
46. Kannan B, Kramer SN. An augmented Lagrange multiplier based method for mixed integer discrete continuous optimization and its applications to mechanical design. 1994.
47. Dasgupta D, Michalewicz Z. *Evolutionary Algorithms in Engineering Applications*. Springer Science & Business Media; 2013.
48. American Society of Civil Engineers. *Minimum Design Loads and Associated Criteria for Buildings and Other Structures*. American Society of Civil Engineers; 2017.
49. American Concrete Institute. *Building Code Requirements for Structural Concrete (ACI 318-11)*. American Concrete Institute; 2011.
50. Hammond G, Jones C. *Inventory of Carbon & Energy: ICE*. Vol. 5. Sustainable Energy Research Team, Department of Mechanical Engineering; 2008.